Int. J. Heat Mass Transfer. Vol. 15, pp. 115–125. Pergamon Press 1972. Printed in Great Britain

FLOW EFFECTS ON BUBBLE GROWTH AND COLLAPSE IN SURFACE BOILING

A. H. ABDELMESSIH, F. C. HOOPER and S. **NANGIA**
Department of Mechanical Engineering. University of Toronto, Toronto 5, Canada

(Received 24 August 1970 and in revised form 3 May 1971)

Abstract-High speed photography was used to investigate the effect of fluid velocity on the growth and collapse of vapor bubbles in slightly subcooled distilled water in an open loop.

Profile pictures of vapor bubbles at a magnification of about 2 × on the film were made at about 7000 frames per s, over a range of water velocities from 3 to 7·5 ft/s, and heat fluxes from 5.94×10^4 to $1{\cdot}46 \times 10^5$ Btu/hft^2, with subcooling of 3·5 F". This corresponds to a Jakob number (at T_{sat}) of 5·5.

The photographic results showed the bubbles being ejected from the nucleation site and collapsing in the subcooled main stream. This study showed an increase in fluid velocity resulted in a decreased bubble size and life span, whereas an increase in the heat flux resulted in an increased bubble size and life span. The fluid velocity did not show any effect on the frequency of formation of bubbles but, up to a limiting value, an increase in the heat flux resulted in an increase in the bubble frequency at a given site.

NOMENCLATURE

A, surface area ;
C. specific heat (constant pressure) ;
f, Frequency ;
h_{fg}, latent heat of vaporization ;
Ja, Jakob number = $(\rho_L C \Delta T/\rho_v h_{fg})$, $\Delta T = T_{sat} - T_b$,
m, vapor bubble growth constant defined by $R = mt^{\frac{1}{2}}$;
N_{Re}, Reynolds number ;
P, pressure ;
ΔP, pressure differential between bubble interior and surroundings ;
q, heat flux ;
q/A, heat flux density ;
R, radius of bubble ;
$\dot{R}$, velocity of vapor–liquid interface, dR/dt ;
R_m, maximum bubble radius ;
R_0, initial bubble radius ;
t, time ;
t_H, dimensionless time;
t_m, maximum growth time:
T, temperature;
T_b, bulk temperature;
T_w, heater temperature;
ΔT, temperature difference ;
V, velocity ;
Y, dimensionless radius $= R/R_m$;
α, thermal diffusivity ;
ρ, density.

Subscripts
L, liquid ;
max, maximum;
sat, saturation.
v, vapor.

INTRODUCTION

generation, obtained with surface boiling are associated with bubble growth and collapse. The bubble dynamics in a subcooled liquid were investigated experimentally by Gunther and Kreith [1] and by Ellion [2] in non-flow systems and by Gunther [3] in a flow system. They studied the bubble growth and collapse under highly subcooled conditions in degassed liquids and observed that the bubbles, roughly hemispherical in shape, remained attached to the heating surface while they grew and collapsed at frequencies higher than 1000 cycles per second. The problem has also been investigated analytically. Zuber [4] equated the transient heat conduction from the liquid boundary layer at the bubble interface to the increase in the latent heat of the bubble plus the heat transfer from the boundary layer to the bulk liquid, and derived equation (1) which predicts the growth and collapse of vapor bubbles in a subcooled liquid pool.

$$R/R_m = (t/t_m)^{\frac{1}{2}}\left[2 - (t/t_m)^{\frac{1}{2}}\right] \tag{1}$$

Bankoff and Mikesell [5] analyzed bubble growth and collapse, considering the effects of liquid inertia only.

Florschuetz and Chao [6] investigated the collapse of a vapor bubble under near zero gravity conditions and suggested that the collapse modes could be classified into three categories. For their first category, liquid inertia controlled collapse, they obtained an expression similar to that of Bankoff and Mikesell. For the case when heat transfer is the controlling factor, they obtained the expression:

$$3t_H = 2\frac{R_0}{R} + \left(\frac{R}{R_0}\right)^2 - 3 \tag{2}$$

where

$$t_H = \frac{4}{\pi}(Ja)^2\frac{\alpha t}{R_0^2}$$

For the third or intermediate case, where both liquid inertia and heat transfer are of importance, they defined a new dimensionless parameter,

$$B = (Ja)^2(\alpha/R_0)(\rho_L/\Delta P)^{\frac{1}{2}} \tag{3}$$

which characterized the relative importance of heat transfer and liquid inertia in the spherically symmetrical collapse of vapor bubbles.

Florschuetz and Chao did not take into account translational velocity of a bubble, since they investigated the bubble collapse under free fall conditions. Wittke and Chao [7], on the other hand, included the effect of translational velocity of the bubble in their analysis of vapor bubbles collapsing in a subcooled liquid. They investigated the case when heat transfer was the controlling mechanism and observed that the faster the bubble translated the more rapidly it collapsed.

Recently Cho and Seban [8] presented a numerical analysis of the collapse of a vapor bubble due to a sudden increase in the system pressure. They included the motion of the vapor in the bubbles, which Florschuetz and Chao assumed to be negligible, and predicted that the bubbles should oscillate as they collapse and that the oscillations should become more pronounced as the subcooling increases. This was also indicated by Theofanous *et al.* [9].

Experimental data in subcooled flow boiling are almost nonexistent and consequently this study was undertaken to obtain some data on the growth and collapse of water vapor bubbles in flow boiling.

EXPERIMENTAL APPARATUS AND PROCEDURE

The experimental apparatus is shown schematically in Fig. 1. It is basically an open or vented system consisting of a pump, flow meter, heater, test section, condenser, and connecting piping. It is fully described elsewhere [10, 11]. Figure 2 shows a view of the test section.

The test element used in this case was a flat electrical heating strip, insulated on its undersurface. It consisted of a stainless steel strip, 0·25 in. wide, 0·006 in. thick, cut to a length of 2·25 in., and fastened by a small screw at either end to rectangular copper bars. This element was mounted concentrically in the 0·824 in. dia. test section. The lower, or upstream end of the heater was transisted into a cone at its leading edge. This entry arrangement permitted the development of the thermal and flow boundary layers ahead of the observed nucleation site.

The temperature of the under surface of the stainless steel strip was measured by means of a 36 gauge teflon coated copper–constantan thermocouple junction separated from the strip by a thin polyester electrically insulating film.

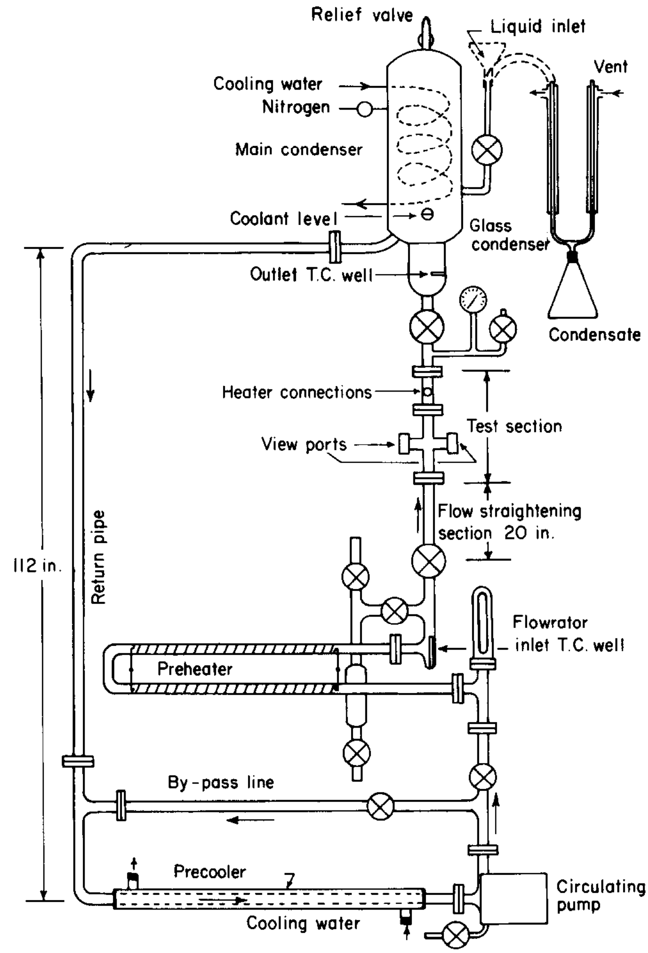

FIG. 1. Forced convection test loop.

Nucleation site

The top surface of the heating strip was smoothed by very fine grade emery cloth, and a small depression of approximately 0·007 in. dia. at the mouth was made with a carboloy needle. All observations were made on bubbles nucleating from this artificial site. A coating of Bordens' clear epoxy cement was then applied over the underside of the strip in order to prevent bubble nucleation from the bottom of the strip. After the assembly of the test element was com-completed the surface of the stainless steel strip was thoroughly cleaned with acetone and distilled water.

High speed photography

A 16 mm "Hycam" camera was used at a framing rate of approximately 7000 frames/s to observe bubble growth and collapse.

Illumination was provided by a single 650 W photo spotlight, placed about 10 in. from the rear window. This type of backlighting was found to give good contrast so that the bubble outlines were clearly defined. A timing light generator was used to provide timing marks on the film.

A total of 50 reversal films, each of 100 ft length was used in this investigation. Thirty-four of the films were used to record controlled

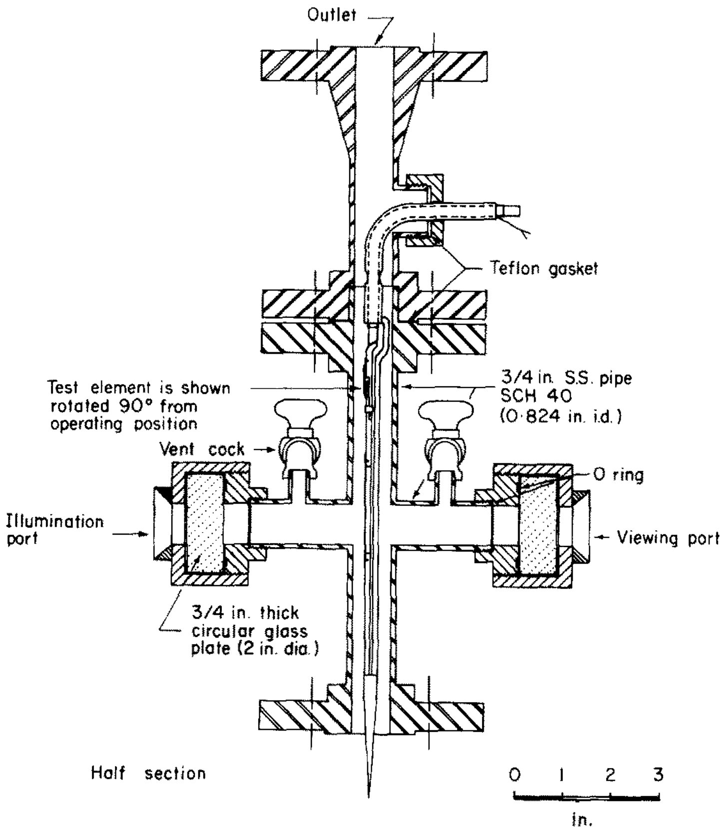

FIG. 2. Details at the test section.

boiling conditions, while the remaining 16 were used for preliminary work.

Motion picture analysis

(i) *Zero time.* Zero time is defined as the frame prior to the first appearance of a bubble on the film. The error introduced by this assumption is less than 0·14 ms.

(ii) *Bubble diameter measurements.* The films were analysed frame by frame on a microfilm reader with a magnification of 40 ×. The bubbles were assumed to be ellipsoidal in shape with their principal axes perpendicular to the line of sight, and the bubble diameter was defined as the geometric mean of the principal diameters.

RESULTS AND DISCUSSION

Photographic observations

A typical sequence of bubbles growing and departing from the heated surface and collapsing in the subcooled flow is shown in Fig. 3. The Reynolds number is based on the equivalent diameter of the annular test section. All results reported here are for distilled water.

Following nucleation, the bubbles which are approximately hemispherical in shape, grow above the nucleating site. As the bubble size increases, the shape of the bubble, due to the influence of the shearing flow near the surface, changes from hemispherical to oblate, with the major axis inclined to the heater surface, as shown in frames 3 and 4 of Fig. 3. A bubble

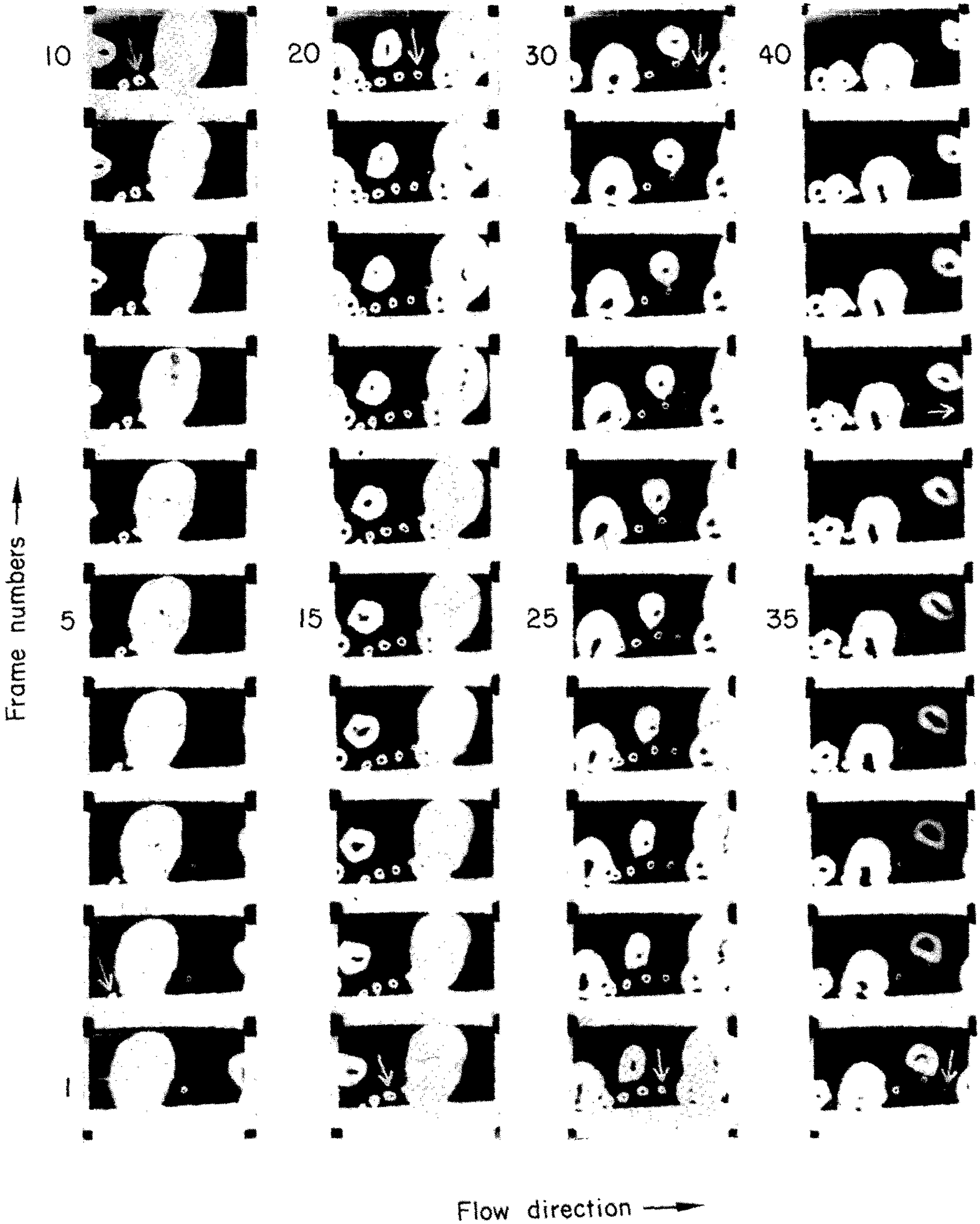

FIG. 3. Frame by frame sequence of typical bubble growth and collapse. Framing speed 6500 fps, $q/A = 5{\cdot}94 \times 10^4$ Btu/hft², $V = 3{\cdot}0$ ft/s.

eventually leaves the site and begins to slip along the heater surface while still attached to it. As it grows further the shape becomes that of an inverted pear with the lower face slipping on the surface in the direction of the flow. Finally, the bubble departs from the surface and its form changes to that of an ellipsoid.

It appears from the photographs as if the bubbles are being projected from the vertical heated surface with a certain velocity. This effect, which is in some ways similar to that reported by Ellion [2] for pool boiling, is undoubtedly influenced by both the liquid inertia and, in this case also by the drag-produced velocity gradient.

The photographs also indicate that the nucleation and bubble growth from a given nucleating site is a periodic process. Following the departure of a bubble from the nucleating site, cooler liquid from the boundary floods back to the site and is heated during a contact or waiting time t_c, at the end of which another bubble is nucleated from the same site. This new bubble grows until at time t_d it in turn departs from the nucleating site and the cycle is repeated. The frequency of bubble emission is then given by $f = 1/(t_c + t_d)$.

At the low value of heat flux of $5{\cdot}94 \times 10^4$ Btu/h ft^2 and a liquid velocity of 3 ft/s, ($N_{Re} = 4{\cdot}66 \times 10^4$) the waiting time was of the order of 0·3 ms and the growth time was of the order of 0·6 ms. As the liquid velocity was increased the waiting time increased but the growth time decreased, resulting in the frequency remaining more or less constant at about 1100 bubbles per s. At higher values of heat fluxes ($1{\cdot}3 \times 10^5$ and $1{\cdot}46 \times 10^5$ Btu/hft^2) both the waiting time and the growth time remained more or less constant, and of the order of 0·3 ms each, within the velocity range investigated, and the frequency was found to increase to about 1700 bubbles/s. This indicated that at higher values of heat fluxes the effect of increasing the heat flux was somehow offset, possibly by an increase in the number of active nucleating sites, or by an increase in the average bubble size. The observations suggest that the latter may be of greater importance in the range of heat fluxes investigated in the present work.

Bubble growth and collapse data

From each of the 34 films ten bubbles nucleating from the same cavity were measured. From these, bubbles representing typical behavior were selected, and the data were plotted as shown in Fig. 4.

Figure 4 shows bubble growth and collapse at a constant heat flux of $1{\cdot}3 \times 10^5$ Btu/hft^2 and a liquid subcooling of 3·5F°, while the liquid velocity varies from 3·75 to 6 f/s (N_{Re} from $5{\cdot}82 \times 10^4$ to $9{\cdot}32 \times 10^4$). The velocity range selected was such that the bubbles nucleating from the artificial site were clearly visible on the film. At a velocity higher than 6 f/s the artificial nucleating site became inactive. At a velocity lower than 3·75 f/s for this particular heat flux, it became impossible to take pictures of the bubbles nucleating from the chosen site due to its being obscured by other bubbles nucleating from neighboring sites.

The values of heat fluxes used in this investigation were not very high, as at higher values of heat flux the bubble population increased and again obscured the view of the nucleating site.

These results reveal that the initial bubble growth is very rapid, but as the size increases the growth rate slows and the bubble attains a maximum diameter. The initial rapid growth could be attributed to the bubble growing on the surface, deriving heat both from the heated surface through a microlayer, as described by Cooper [12] and by Sernas and Hooper [13] for pool boiling, and from surrounding superheated liquid. This corresponds to the initial steep portion of the bubble growth curves. Due to this rapid initial growth, the temperature of the surrounding liquid and of the heater surface decreases, thus affecting the bubble growth rate. Moreover, as the bubble size increases, the top of the bubble protrudes into the sub-cooled region. Under these conditions

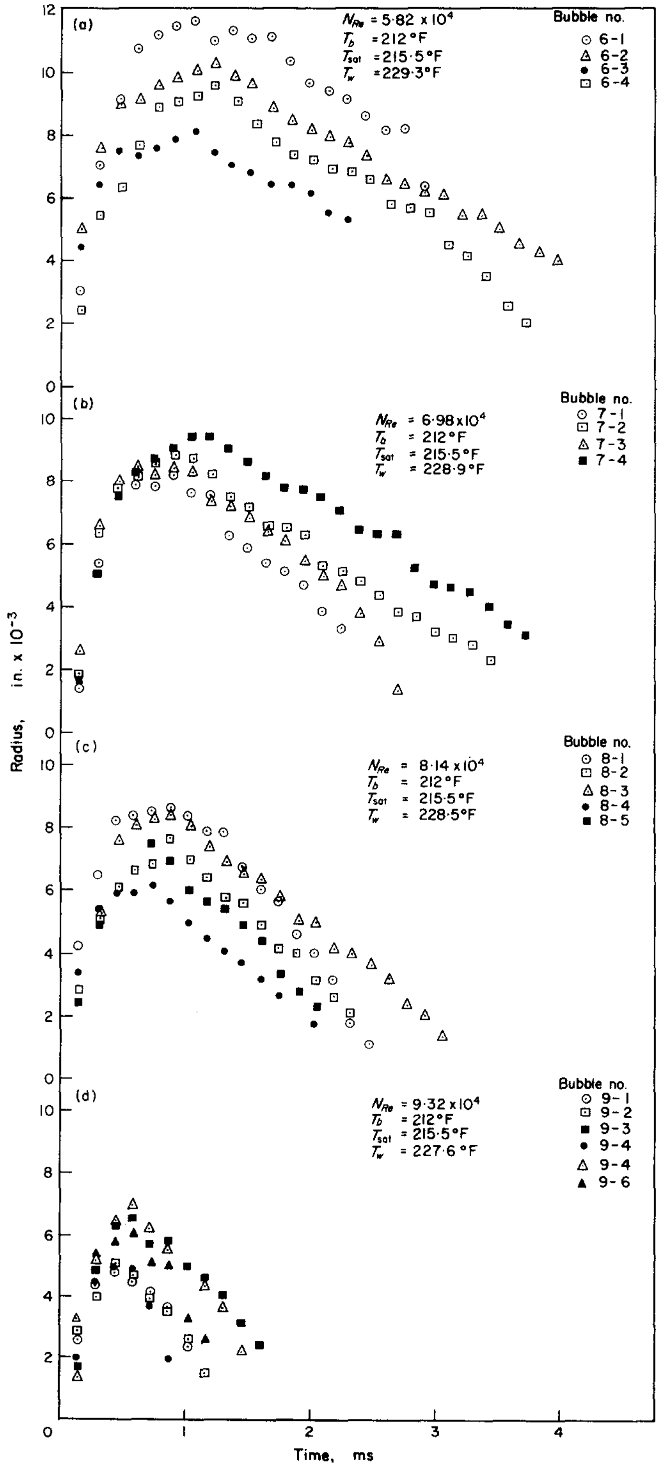

FIG. 4. Bubble growth and collapse at a heat flux of $q/A = 1{\cdot}3 \times 10^5$ Btu/hft², Ja (at T_{sat}) = 5·5, ΔT = 3·5°F.

evaporation occurs at the base of the bubble while condensation takes place at the top interface, thus contributing to a decrease in the overall bubble growth rate. Eventually, when the evaporation rate and the condensation rate become equal, there will be no net flow of vapor into the bubble and the bubble will have attained a maximum diameter, and will depart from the heated surface and start collapsing in the main stream.

Similar sets of curves were produced for heat fluxes of $5{\cdot}94 \times 10^4$ and $1{\cdot}46 \times 10^5$ Btu/hft^2 which show that with increasing heat flux both the maximum bubble diameter and the bubble life span increase, whereas the collapse rate of the bubbles remains more or less constant.

During the collapse phase the plotted data points reflect an oscillatory behaviour of the bubbles which is more pronounced in some cases than in others. The bubble partially collapses and then slows, or even reverses and grows slightly before the collapse continues. Previous authors [6, 9] have observed a similar behavior in pool boiling and attributed it to varying rates of condensation corresponding to varying vapor pressure at the bubble wall. Hooper *et al.* [14] have reported an analogous behavior for growing bubbles.

The observations have shown that even though the bubbles are nucleating from the same site and under the same boiling conditions, both the maximum radii and the life spans of the bubbles vary. These variations are more pronounced in some cases than in others. The largest bubble radius observed was 18 per cent above the mean of the maxima for that test. This could be attributed to the microscopic eddies which exist in the liquid. Owing to this variation in maximum bubble radius, an average bubble from each film was selected for purposes of comparison. Plots of typical bubbles selected from those in Fig. 4, showing the effect of fluid velocity on bubble growth and collapse, are reproduced in Fig. 5.

Effect of liquid velocity

It is clear from Fig. 5 that both the maximum bubble radius and the bubble span decrease as the liquid velocity increases. At the lower velocity the time of collapse from the maximum radius is much greater than the growth time, but as the velocity increases, the collapse time

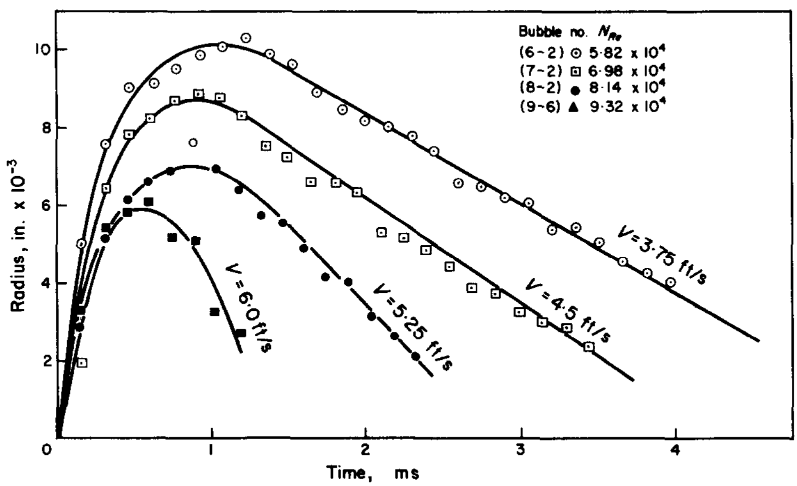

FIG. 5. Effect of liquid velocity on bubble growth and collapse at a heat flux of $q/A = 1{\cdot}3 \times 10^5$ Btu/hft^2.

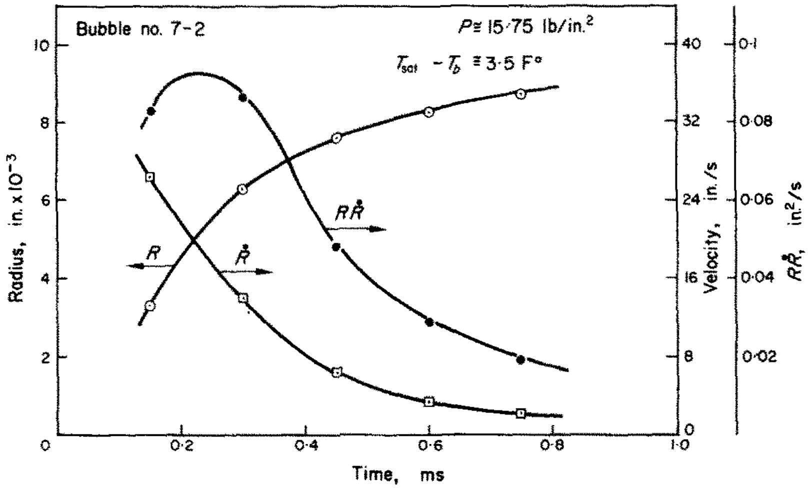

FIG. 6. Measured values of bubble radius R and calculated values of $\dot{R}$ and $R\dot{R}$ shown as functions of time for the growth period of a typical bubble. $q/A = 1{\cdot}3 \times 10^5$ Btu/hft², $N_{Re} = 6{\cdot}98 \times 10^4$.

relative to the growth time decreases, and eventually the collapse curves become quite steep and are very nearly mirror images of the growth curves, suggesting an increasing inertial domination.

The decrease in both maximum bubble radius and bubble life span as a result of an increase in liquid velocity could be attributed to the corresponding increase in turbulence. Increased turbulence of a stream, caused by an increase in the shear stress at the boundary, results in a decrease of the thickness of the thermal boundary layer. Consequently, the surface temperature and the boundary layer superheat decrease and the bubble grows to a smaller maximum radius. Because the increased turbulence increases the heat transfer rate at the bubble wall the collapse rate of the bubbles also increases.

R, $\dot{R}$ and the product $R\dot{R}$ during bubble growth

A typical plot of the radius R, the bubble wall velocity $\dot{R}$ and the product $R\dot{R}$ is shown in Fig. 6.

Figure 6 shows that $\dot{R}$ decreases as the bubble radius increases. It is well known that the product $R\dot{R}$ is a constant for the asymptotic growth of vapor bubbles in pool boiling. However, it is clear in this study that the product $R\dot{R}$ decreases as the bubble radius increases, except for a short duration at the start of bubble growth. This indicates that the bubbles do not follow the asymptotic growth relation of the form $R = mt^{\frac{1}{2}}$, and suggests that the curve $R\dot{R}$ starts sloping downward when the bubble tops have penetrated into the subcooled region resulting in a slowing of the growth rate due to condensation at the top of the bubble.

Comparison of experimental data with available theoretical models

Figure 7 is a plot of dimensionless radius versus dimensionless time for the four bubbles shown in Fig. 5, together with equation (1). The agreement between the experimental data and Zuber's equation seems to be quite reasonable in the growth period. However, the collapse rate predicted by Zuber [4] is slightly faster than that observed in the experimental data at low velocities. In addition, the plots also reveal

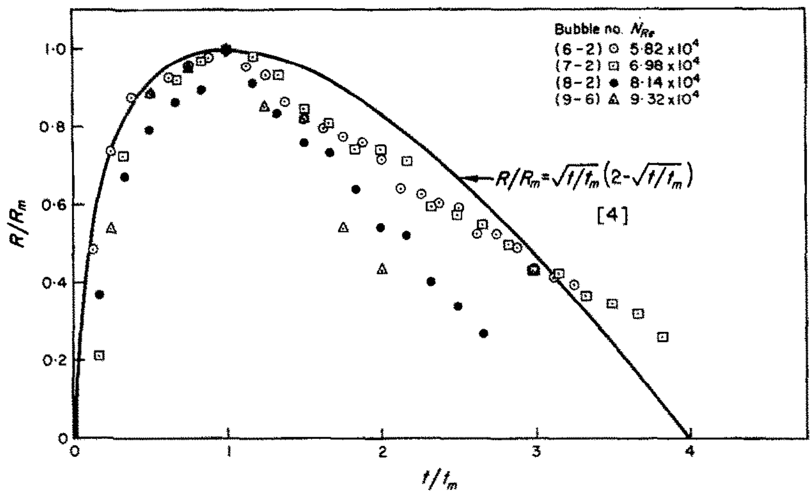

FIG. 7. Dimensionless bubble growth and collapse data compared with Zuber's equation. $q/A = 1{\cdot}3 \times 10^5$ Btu/hft^2.

that the collapse rate of the bubbles increases as the liquid velocity increases.

The results of this investigation suggest that, at low subcooling and low flow velocities, the bubble collapse is mainly controlled by heat transfer and could be approximated by equation (1). However, at higher flow velocities other effects such as turbulence and inertia apparently become increasingly dominant, and the collapse curve deviates from equation (1).

In Fig. 8 data are plotted for the collapse phase of the four bubbles shown in Fig. 5, in terms of the dimensionless radius versus a dimensionless time, together with equation (2). Again the collapse rate predicted by equation (2) is slower than the actual collapse rate

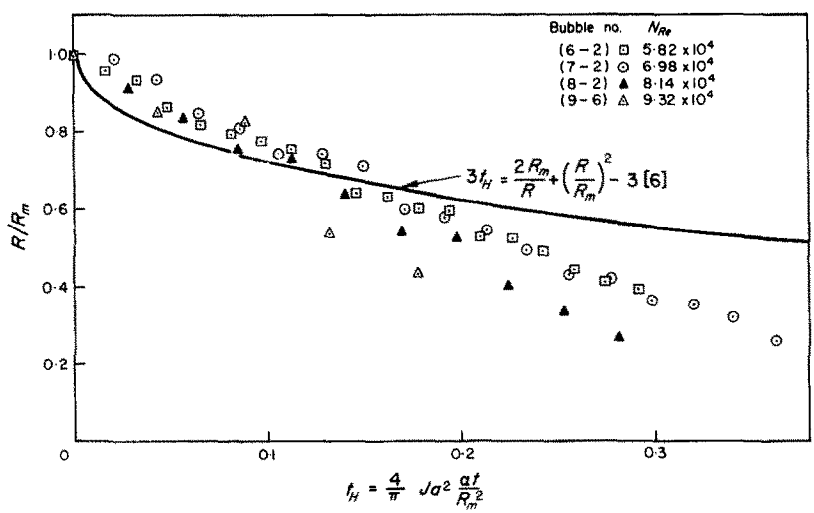

FIG. 8. Dimensionless bubble collapse data compared with the Florschuetz and Chao equation. $q/A = 1{\cdot}3 \times 10^5$ Btu/hft^2.

observed in the experiments. The difference is probably due to the effect of liquid velocity and the consequent increase in the rate of heat transfer at the bubble interface due to increased turbulence.

Florschuetz and Chao in deriving equation (2) did not take into account the effect of liquid velocity on the bubble collapse. Furthermore, they made use of the Plesset–Zwick temperature integral, thus assuming the presence of a thin thermal boundary layer around the bubble, and hence their solution is valid only for large Jakob numbers. For small values of Jakob numbers, as is the case in this investigation, the thin thermal boundary layer approximation breaks down and a deviation would be expected between equation (2) and the present experimental results. This was also pointed out by Wittke and Chao [7].

CONCLUSIONS

The photographic observations show that the bubbles at the time of departure are ejected like projectiles from the nucleating site and collapse in the main stream.

It has been observed that the effect of an increase in liquid velocity was to decrease the bubble population, the bubble size and life span, whereas the effect of an increase in heat flux was to increase the bubble population, the bubble size and life span over the range of heat fluxes and liquid velocities employed in this investigation.

The velocity did not have any effect on the frequency of formation of bubbles at a given site, but with increasing heat flux the frequency increased and finally became constant.

During the collapse phase the plotted data reflect an oscillatory behavior of the bubbles. A similar behavior in pool boiling has also been observed by various other investigators. The results also show that the collapse rate of the bubbles increases as the liquid velocity increases.

The agreement between the experimental data and Zuber's analytical equation was reasonable for the growth period, but an increasing deviation was observed with increasing liquid velocities in the collapse range.

The experimental results also show that the collapse rate for vapor bubbles in flow boiling is, as might be expected, faster than the rate predicted by the Florschuetz and Chao equation for free fall conditions.

ACKNOWLEDGEMENT

The authors wish to acknowledge the financial support provided by the National Research Council of Canada.

REFERENCES

1. F. C. Gunther and F. Kreith, Photographic study of of bubble formation in heat transfer to subcooled water, Prog. Rept. No. 4-120, Jet Prop. Lab., Cal. Inst. Tech. (March 1950).
2. M. E. Ellion, A study of the mechanism of boiling heat transfer, Memo No. 20–88 Jet Prop. Lab., Cal. Inst. Tech. (1954).
3. F. C. Gunther, Photographic study of surface boiling heat transfer to water with forced convection, *Trans. Am. Soc. Mech. Engrs* **73**, 115–123 (1951).
4. N. Zuber, Hydrodynamic aspects of boiling heat transfer, USAEC Rep. AECU-4439, Ph.D thesis, Univ. of California, Los Angeles (1959).
5. S. G. Bankoff and R. D. Mikesell, Bubble growth rates in highly subcooled nucleate boiling, *Chem. Engng Prog. Symp. Ser.* No. 29 (1959).
6. L. W. Florschuetz and B. T. Chao, On the mechanics of vapor bubble collapse, *J. Heat Transfer* **87**, 209–220 (1965).
7. D. D. Wittke and B. T. Chao, Collapse of vapor bubbles with translatory motion, *J. Heat Transfer* **89**, 17–24 (1967).
8. S. M. Cho and R. A. Seban, On some aspects of steam bubble collapse, ASME Paper No. 69-HT-F (1969).
9. T. G. Theofanous, L. Biasi, H. S. Isbin and H. K. Fauske, Nonequilibrium bubble collapse—a theoretical study, A.I.C.E. Preprint 1, Eleventh National Heat Transfer Conference, Minneapolis (Aug. 1969).
10. V. Sernas, A test facility for the determination of burnout heat flux in flowing organic mixtures, M.A.Sc. Thesis, Mech. Eng. Department, University of Toronto (1964).
11. S. Nangia, The effect of flow on bubble growth and collapse in surface boiling, M.A.Sc. Thesis, Mech. Eng. Department, University of Toronto (1970).
12. M. G. Cooper and A. J. P. Lloyd, Transient local heat flux in nucleate boiling, Proc. 3rd Int. Heat Transfer Conf., Chicago (1966).
13. V. Sernas and F. C. Hooper, The initial vapor bubble growth on a heated wall during nucleate boiling, *Int. J. Heat Mass Transfer* **12**, 1627–1639 (1969).
14. F. C. Hooper, G. Faucher and A. Eidlitz, Pressure effects on bubble growth in the flashing of superheated water, Proc. 4th Int. Heat Transfer Conf., Paris (1970).

EFFETS DE L'ECOULEMENT SUR LA CROISSANCE ET LA DISPARITION DES BULLES DANS L'ÉBULLITION EN SURFACE

Résumé—La photographie ultra-rapide est utilisée pour étudier l'effet de la vitesse du fluide sur la croissance et la disparition des bulles de vapeur pour l'eau distillée et légèrement sous-refroidie dans une boucle ouverte. Des images des bulles de vapeur ont été obtenues avec un grossissement d'environ 2 *X* sur le film, à 7000 vues par seconde, pour une gamme de vitesse d'eau allant de 1 à 2,25 m/s, des flux thermiques compris entre $1{,}88 . 10^3$ et $4{,}63 . 10^3$ kW/m^2 et avec un sous-refroidissement de 1,94°C. Ceci correspond à un nombre de Jacob (à T_{sat}) égal à 5,5.

Les résultats photographiques montrent les bulles sortant des sites de nucléation et s'évanouissant dans l'écoulement principal sous-refroidi. Cette étude montre qu'un accroissement de la vitesse du fluide s'accompagne d'une diminution de la taille et de la durée de vie des bulles. La vitesse du fluide ne semble pas avoir d'effet sur la fréquence de formation des bulles mais, jusqu'à une certaine limite, une augmentation du flux thermique provoque un accroissement de la fréquences des bulles à un site donné.

STRÖMUNGSEINFLUSS AUF BLASENWACHSTUM UND BLASENZUSAMMENBRUCH BEIM OBERFLÄCHENSIEDEN

Zusammenfassung—Zur Untersuchung des Einflusses der Strömungsgeschwindigkeit auf Wachstum und Zusammenbruch von Dampfblasen in leicht unterkühltem destilliertem Wasser in einem offenen Kreislauf wurde die Hochgeschwindigkeitsphotographie verwendet.

Es wurden Profilaufnahmen von Dampfblasen gemacht mit zweifacher Vergrösserung bei 7000 Bildern/sec. über einen Geschwindigkeitsbereich von 0,9 bis 2,3 m/s und Wärmestromdichten von 18,7 bis 46 W/cm^2, mit 2 K Unterkühlung. Dies entspricht einer Jakobs-Zahl (bei T_{satt}) von 5,5.

Die photographischen Ergebnisse zeigten, dass die Blasen von den Keimstellen ausgeworfen werden und in dem unterkühlten Hauptstrom zusammenbrechen. Die Untersuchung ergab, dass ein Anstieg der Flüssigkeitsgeschwindigkeit eine Verkleinerung der Blasengrösse und der Lebensdauer zur Folge hat, während ein Anstieg der Wärmestromdichte Blasengrösse und Lebensdauer ansteigen liess. Die Flüssigkeitsgeschwindigkeit zeigte keinen Einfluss auf die Blasenfrequenz, aber bis zu einem bestimmeten Wert hatte ein Anstieg der Wärmestromdichte ein Anwachsen der Blasenfrequenz bei bestimmter Grösse zur Folge.

ВЛИЯНИЕ ТЕЧЕНИЯ НА РОСТ И РАЗРЫВ ПУЗЫРЬКОВ ПРИ КИПЕНИИ НА ПОВЕРХНОСТИ

Аннотация—Использовалась скоростная фотосъемка для исследования влияния скорости жидкости на рост и разрыв пузырьков пара в слегка недогретой дистиллированной воде в открытой петле.

Профильные снимки пузырьков пара при увеличении в 2X раза на пленке производились со скоростью 7,000 кадров в секунду в диапазоне скоростей воды от 3 до 7,5 фут/сек., и плотностях теплового потока от $5{,}94 \times 10^4$ до $1{,}46 \times 10^5$ Btu/h.ft^2, при недогреве в 3,5°F. Это соответствует числу Якоба (при T_{HAC}) равному 5,5.

На фотоснимках показаны пузырьки, покидающие место зарождения и разрывающиеся в недогретом основном потоке. Это исследование показало увеличение скорости жидкости, в результате чего уменьшился размер пузырьков и время их жизни, в то время как увеличение теплового потока привело к увеличению размера пузырьков и времени их жизни. Скорость жидкости не показала какого—нибудь влияния на частоту образования пузырьков, но в результате увеличения теплового потока увеличилась до определенного значения частота пузырьков в данном месте зарождения.